Site Isolation in Phosphorescent Bichromophoric Block Copolymers Designed for White Electroluminescence

By *Daniel A. Poulsen, Bumjoon J. Kim, Biwu Ma, C. Sebastian Zonte,* and *Jean M. J. Fréchet**

White organic light-emitting diodes (WOLEDs) have attracted great attention for their potential use in full color displays and solid-state lighting applications due to several advantages, such as low cost and flexibility. To date, the most efficient WOLEDs have used small phosphorescent molecules in multilayer structured devices prepared by high vacuum vapor deposition. The key issue in these systems is that the phosphorescent emission produced by each individual metal complex Ir(III) or Pt(II),[1,2] is narrow, thus requiring simultaneous emission from more than one color phosphor to illuminate across the visible region. Typically this is achieved through a combination of either three different chromophores emitting blue, green, and red, or of two different ones emitting green/blue and orange/red. If more than one phosphorescent emitter is present in a device, the electroluminescent color may be affected by the energy transfer (both Förster and Dexter) between emitters. Vapor deposition enables isolation of the various emitters to minimize the energy transfer and achieve the desired goal of multiple emission using techniques such as patterning,[3] stacking,[4,5] layered isolation,[6,7] and exciton management.[8]

Because polymeric materials can be solution-processed, they constitute an interesting option for application in OLEDs due to their potential to reduce cost and increase scalability. Another advantage is that a single polymer chain can bear multiple functional groups, each contributing to the tuning of properties. For example, successful demonstrations of polymer WOLEDs have been based on blends of fluorescent polymers,[9] polymers incorporating multiple fluorescent emitters in their side chains[10,11] or their backbone[12,13] and fluorescent polymers doped with small molecule phosphorescent emitters.[14–16] However, these devices are generally fluorescent systems with limited internal quantum efficiencies or doped phosphorescent systems with poor stability. Furthermore, the occurrence of energy transfer limits the amount of low energy dopant that can be incorporated into these polymers, which affects their intrinsic efficiency.[17–19] There have been some efforts to suppress this energy transfer using dendrimers for site isolation,[20,21] but ultimately multilayer structures that can isolate phosphorescent emitters are needed. Unfortunately, this is extremely difficult to achieve with solution processing as the deposition of a layer must not affect any previously deposited layers.

Block copolymers allow hierarchical supramolecular control over the spatial location of their functional component blocks as well as various nanoscale objects.[22–26] This design flexibility has been exploited in the efficient fabrication of novel functional materials, such as nanostructured solar cells, photonic bandgap materials, highly efficient catalysts, and high-density magnetic-storage media.[27–31] Therefore, block copolymers have the unique potential to spontaneously achieve phosphorescent emitter isolation through self-assembly. Herein, we have explored their use as active materials for WOLEDs in which phosphorescent emitter isolation can be achieved. We have exploited the use of triarylamine (TPA) oxadiazole (OXA) diblock copolymers (TPA-*b*-OXA), which have been used as host materials due to their high triplet energy and charge-transport properties enabling a balance of holes and electrons.[32] These coil–coil type TPA-*b*-OXA diblocks can produce various morphologies with controlled domain spacings ranging from 10–50 nm. By incorporating two different colored phosphorescent Ir(III) emitters (green–blue and orange–red emissive pendant styryl heteroleptic Ir(III) complexes) randomly into each different block, we have been able to produce a block-copolymer system, (TPA-*r*-Blue)-*b*-(OXA-*r*-Red), which can deliver site isolation of the two emitters. As a result of site isolation these diblock copolymers can be targeted to suppress energy transfer from high to lower energy emitters, which generally occurs at distances below 10 nm.[33,34] With these block copolymers, we demonstrate a seld-assembled single layer solution processed WOLED that provides improved white color balance, and efficiency. Furthermore, by varying the molecular weight (MW) of (TPA-*r*-Blue)-*b*-(OXA-*r*-Red) and the ratio of blue to red emitters, we have investigated the effect of domain spacing on the electroluminescence spectrum and device performance.

Polymers containing heavy metal complexes have been demonstrated previously for similar Ir(III) complexes through incorporation of ancillary ligand then post polymerization complex formation, or through the post polymerization attachment of preformed Ir(III) complexes.[35,36] Unfortunately, these strategies are unsuitable since they do not allow incorporation of

[*] Prof. J. M. J. Fréchet, D. A. Poulsen, Prof. B. J. Kim, Dr. B. Ma, C. S. Zonte
Materials Science Division, Lawrence Berkeley National Laboratory
University of California
Berkeley, CA 94720-1460 (USA)
E-mail: frechet@berkeley.edu
Prof. J. M. J. Fréchet, D. A. Poulsen, Prof. B. Kim, Dr. B. Ma, C. S. Zonte
College of Chemistry, University of California
Berkeley, CA 94720-1460 (USA)
Prof. B. J. Kim
Department of Chemical and Biomolecular Engineering
Korea Advanced Institute of Science and Technology (KAIST)
Daejeon, 305-701, Korea

DOI: 10.1002/adma.200901453

different colored emitters preferentially in either block without the development of complex orthogonal connection strategies. Other approaches involving the incorporation of heavy metal complexes within the polymer backbone have been accompanied by a significant alteration of the photophysical properties due to extended π-conjugation of the Ir(III) complex in the polymer.[37,38] To overcome these limitations we have designed and synthesized two heteroleptic Ir(III) complexes bearing a pendant styrene handle, which enables their polymerization using ''living'' free radical conditions that do not alter the photophysical properties of the Ir(III) complex, as shown in Scheme 1. In this study, the heteroleptic Ir(III) complexes, $Ir(dfppy)_2(tpzs)$ (**3**) and $Ir(pq)_2(tpys)$ (**4**), which are modified versions of FIrpic[39,40] and $Ir(pq)_2(tpy)$,[41] were designed such that the polymerizable group is both spatially distant and electronically isolated from the Ir(III) center. The polymerizable ancillary ligands, 1-*p*-tolylpyrazole styrene (tpzs) and 2-*p*-tolylpyridine styrene (tpys) have been chosen for their high triplet energy and thus phosphorescent emission color is dictated by the other two lower energy cyclometallating ligands. As a result, **3** and **4** show phosphorescent emission in the green/blue and orange/red region of the visible spectrum, respectively.

In this study the M_n of the polymers was varied with a wide range from 30 to 150 kDa, but the lengths of the two blocks were kept equal in all cases in order to preserve the morphology at different domain spacings thus enabling a fundamental study of the effect of domain spacing on electroluminescence (EL) and device performance. The target (TPA-*r*-Blue)-*b*-(OXA-*r*-Red) block copolymers **5**–**8** were synthesized by living radical polymerization as shown in Scheme 1. Diblock copolymers were obtained by first preparing the first block via a random copolymerization of TPA with **3**, followed by addition of the second block in a random copolymerization of OXA with **4**. The resulting polymers contained 10 wt % of **3** in the TPA block, while the amount of **4** in the OXA block was varied in a series of copolymers to determine the optimal ratio of **3** to **4** (blue to red) emitters leading to white electroluminescence. The weight fraction of **3** (blue monomer) in the TPA block was chosen to avoid triplet-triplet annihilation by high Ir(III) doping while enabling high brightness. The polymers synthesized and used in this study are detailed in Table 1.

Table 1. Summary of synthesized polymers.

	Sample	MW[a]/kDa	PDI	Blue:Red
5a	(TPA-*r*-10B)-*b*-(OXA-*r*-0.1R)	30	1.2	10:0.1
5b	(TPA-*r*-10B)-*b*-(OXA-*r*-0.5R)	30	1.2	10:0.5
6a	(TPA-*r*-10B)-*b*-(OXA-*r*-0.5R)	70	1.3	10:0.5
6b	(TPA-*r*-10B)-*b*-(OXA-*r*-1R)	70	1.4	10:1
7a	(TPA-*r*-10B)-*b*-(OXA)	100	1.4	10:0
7b	(TPA-*r*-10B)-*b*-(OXA-*r*-0.5R)	100	1.4	10:0.5
7c	(TPA-*r*-10B)-*b*-(OXA-*r*-1R)	100	1.4	10:1
8a	(TPA-*r*-10B)-*b*-(OXA-*r*-1R)	150	1.4	10:1
8b	(TPA-*r*-10B)-*b*-(OXA-*r*-2R)	150	1.5	10:2

[a] M_n value measured by SEC MALLS.

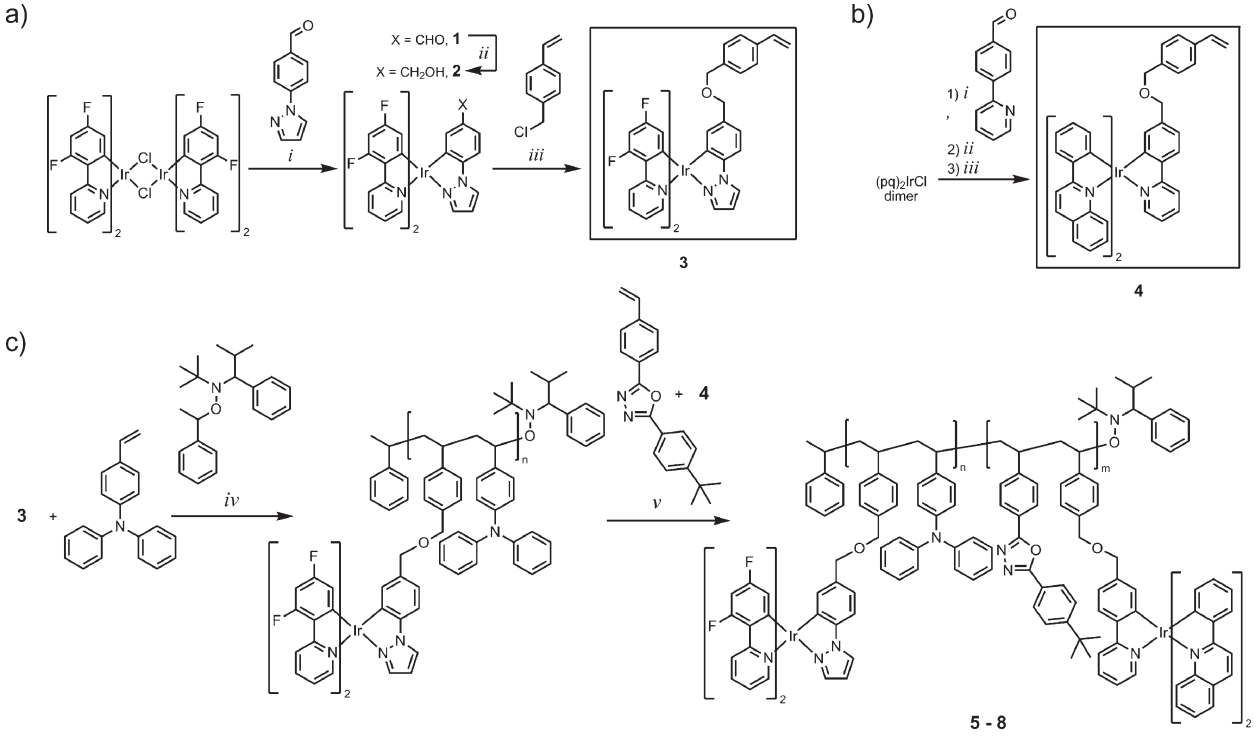

Scheme 1. Monomer synthesis and polymerization: a) synthesis of monomer $Ir(dfppy)_2(tpzs)$ (**3**), b) synthesis of iridium monomer $Ir(pq)_2(tpys)$ (**4**), and c) synthesis of diblock copolymers (**5**–**8**), with the conditions of *i*. diglyme, $AgCF_3SO_4$, 95 °C, 24 h; *ii*. 1:1 DCM: ethanol, $NaBH_4$, RT, 24 h; *iii*. THF, KI, KH, 18-crown-6, RT, 24 h; *iv*, *v*. *t*-butylbenzene, argon filled sealed ampule, 125 °C, 6 h.

order to achieve a near random distribution of the Ir(III) complexes through each polymer chain. The weight percent as well as the compositional distribution of the Ir(III) complexes in each block were analyzed by SEC with triple detection (UV at 404 nm, MALLS and RI). It was found that the weight fraction of components in the monomer feed matched that in the resulting polymer with even distribution of Ir(III) across the mass range of the polymers (Fig. S1 and S2, Supporting Information). ^{1}H NMR analysis of the polymers confirmed incorporation of the Ir(III) monomers in the polymers (Fig. S3, Supporting Information).

We have explored the use of these copolymers as the single active layer in polymer OLED devices to investigate the fundamental effect of both MW and the ratio of blue to red Ir(III) complexes (**B**:**R**) on device performance. Devices were prepared by spin-coating the (TPA-*r*-Blue)-*b*-(OXA-*r*-Red) copolymers from chlorobenzene solution onto ITO substrates, followed by vapor deposition of a LiF/Al electrode. Figure 1 shows the electroluminescence (EL) spectra of (TPA-*r*-Blue)-*b*-(OXA-*r*-Red) polymers having various MW and **B**:**R** ratios. It is clear that increasing MW results in lower emission from the red Ir(III) complex **4**. In particular, a significant decrease in red emission with a concomitant increase in blue emission is seen when the molecular weight is increased from 30 kDa (**5a**) to 70 kDa (**6a**) while keeping the **B**:**R** ratio constant at 10:0.5. Increasing the MW from 70 kDa (**6a**) to 100 kDa (**7b**) leads to a further decrease in red emission. Figure 1b shows a similar trend is same trend for polymers **6b**, **7c**, and **8a** with MW as high 150 kDa containing a higher **B**:**R** ratio of 10:1. It is clear that the use of larger blocks enables a more balanced dual emission at higher red wt % incorporation.

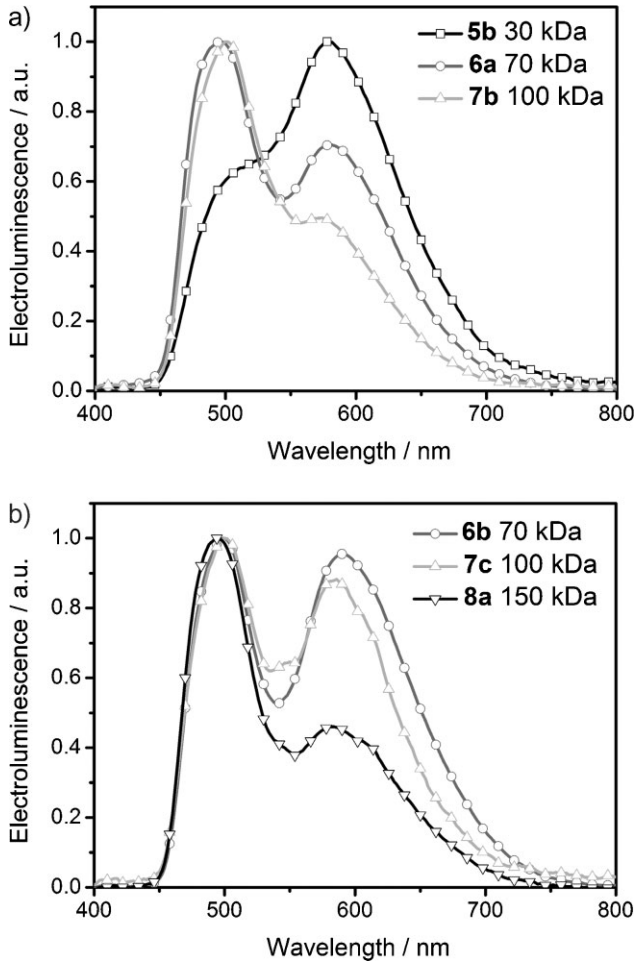

Figure 1. Electroluminescence as a function of molecular weight: a) (TPA-*r*-10 wt % Blue)-*b*-(OXA-*r*-0.5 wt % Red) for three polymers (**5b**, **6a**, **7b**) of increasing MW = 30 kDa, 70 kDa, and 100 kDa; b) (TPA-*r*-10 wt % Blue)-*b*-(OXA-*r*-1 wt % Red) for three polymers (**6b**, **7c**, **8a**) of increasing MW = 70 kDa, 100 kDa, and 150 kDa.

The film morphology of the various (TPA-*r*-Blue)-*b*-(OXA-*r*-Red) copolymers was explored by transmission electron microscopy (TEM) to elucidate the fundamental reason behind the dramatic change in EL with increasing MW. Three different (TPA-*r*-Blue)-*b*-(OXA-*r*-Red) polymers that all show white EL but have different MW values of 30 kDa (**5b**), 100 kDa (**7c**) and 150 kDa (**8b**), respectively, were chosen for this TEM analysis. The samples were annealed at 230 °C for 3 days and slowly cooled and equilibrated at 190 °C for 1 day, which is above the glass transition temperatures of both the TPA (~125 °C) and OXA (~182 °C) polymers.[32] Samples were microtomed to produce 50-nm-thick films, then stained with RuO_4 vapor to enhance the contrast between the (TPA-*r*-Blue) and (OXA-*r*-Red) blocks. The TEM images of Figure 2a–c show the morphology of copolymers **5b**, **7c**, and **8b**. Of particular interest are the clear nanometer-sized fingerprint features characteristic of a lamellar morphology observed in Figure 2b and 2c for films of **7c** and **8b** at MW 100 kDa and 150 kDa, respectively. In contrast, copolymer **5b** with its lower MW of 30 kDa shows no domains, indicating that the film is homogeneous and that the blocks are not phase separated. This coincides with the requirement of far less red iridium monomer for the lower molecular weight polymer **5b** to yield the same EL as the phase separated higher molecular weight polymer **7c**. The dramatic difference in EL between **5b** (MW = 30 kDa) and **7d** (MW = 100 kDa) shown in Figure 1 can be explained by this contrast in nanoscale morphology where the phase separated

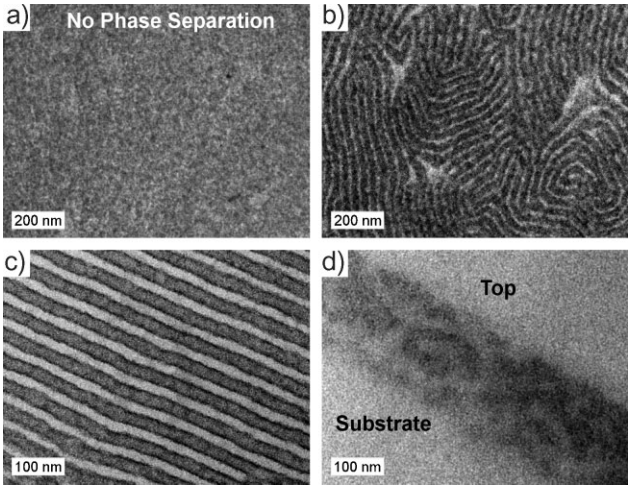

Figure 2. TEM images of (TPA-*r*-Blue)-*b*-(OXA-*r*-Red) polymers having different MW at near equilibrium morphologies: a) **5b** MW = 30 kDa B:R = 10:0.5; b) **7c** MW = 100 kDa B:R = 10:1; c) **8b** MW = 150 kDa B:R = 10:2; d) shows the cross-sectional view of polymer **8b** MW = 150 kDa kDa B:R = 10:2 in thin film as spun cast from chlorobenzene solution.

Table 2. Observed domain spacings.

	Sample	MW[a]/kDa	*d* (GISAXS)[b]/nm	*d* (TEM)[c]/nm
5b	(TPA-*r*-10B)-*b*-(OXA-*r*-0.5R)	30	no phase separation	no phase separation
6b	(TPA-*r*-10B)-*b*-(OXA-*r*-1R)	70	26.5	–
7b	(TPA-*r*-10B)-*b*-(OXA-*r*-0.5R)	100	40.7	36
8a	(TPA-*r*-10B)-*b*-(OXA-*r*-1R)	150	48.3	47

[a] M_n value measured by SEC MALLS. [b] As spuncast from chlorobenzene. [c] Annealed to equilibrium morphology.

domains in **7d** can suppress the energy transfer from blue to red Ir(III) complexes by isolating one from the other. The length scale of domain separation in **7d** (~36 nm) is larger than typical values for energy transfer (<10 nm).[33,34] As MW increases further to 150 kDa, the degree of segregation between the different blocks increases and thus a larger domain spacing of 47 nm is found (Table 2). This is consistent with the theoretical prediction $d \sim M_n^{2/3}$ where d is the spacing between lamellar domains.[42] Therefore, on average, the blue Ir(III) complexes are even further segregated from red ones in films of **8b** (150 kDa), thus enabling the use of a higher **B**:**R** ratio of 10:2 to obtain white EL (Fig. S5). Control experiments confirmed that the morphologies of copolymers containing iridium complexes were same as those without the complexes (TPA-*b*-OXA), which indicates that incorporation of 10 wt % Ir(III) monomer has little effect on the chain conformation of the host polymers. Since all EL measurements were made in the form of a thin film spun cast from chlorobenzene, we have also studied the morphology prepared under same conditions. Figure 2d shows the cross-sectional view of a thin film of **8b** (TPA-*r*-Blue)-*b*-(OXA-*r*-Red). Clearly, a phase segregated morphology is still observed in the absence of annealing but it is less ordered than the lamellar morphology of annealed samples.

While TEM can reveal the nanoscale morphology of these polymers, it does not provide precise information on domain spacing for the samples as spun cast. More quantitative data can be obtained using grazing incidence small angle X-ray scattering (GISAXS). The domain spacings of films ''as spun cast'' were obtained as a function of MW from 30 kDa to 150 kDa from peak positions in the in-plane direction of GISAXS images (Table 2). In contrast to the homogeneous morphology of copolymer **5b** (MW = 30 kDa), the higher MW copolymers **6b**, **7c**, and **8b** all show phase segregated morphologies with increased domain spacing of 26.5, 40.7, and 48.3 nm, respectively.

Controlling the nanoscale morphology of the copolymers to obtain phase separated domains is critical to suppress energy transfer from high to low energy dopants by isolating the blue complexes from the lower energy red Ir(III) complexes. The contrast in morphology not only affects the EL, but also other device characteristics. Figure 3 shows the device performance for WOLEDs fabricated from (TPA-*r*-Blue)-*b*-(OXA-*r*-Red) **5a**, **5b** (MW = 30 kDa), and **7c** (MW = 100 kDa). To focus on the effects of MW and morphology on WOLED device performance, these polymers were used as the single active layer in a device with no additional material between anode and cathode. While some dual emission can be obtained even in the absence of phase separated morphologies using very high **B**:**R** ratios (copolymers **5a** and **5b**, Fig. 3a), a much higher proportion of red emitter may be used if phase separation is achieved as in the higher MW **7c** with its 10:1 **B**:**R** ratio. This also affects the external quantum efficiency (EQE) of the device (Fig. 3b) as the higher MW polymer **7c** shows a markedly higher EQE (>1.5%) for white emission than observed with the lower MW polymers **5a** (EQE ~ 0.3%) and **5b** (EQE ~ 0.4%). The data for device brightness is shown for the three different samples in Figure 3c. The device made from the phase separated copolymer **7c** is three times brighter and has lower turn-on voltage than devices made from copolymers **5a** and **5b**. While the absolute value for the brightness of all devices is rather low, due in large part to the poor intrinsic characteristics of the blue emitter, this study demonstrates the effect of phase separation and larger interfacial area on device performance. The large interfacial area between hole and electron transporting domains facilitates hole-electron recombination and thus produces a higher EQE.[32] However, if the MW of the blocks is increased to improve chromophore isolation beyond a certain threshold the interfacial area will decrease thus negating the benefit of site isolation.

In order to confirm that the improvement in device performance for the higher MW (TPA-*r*-Blue)-*b*-(OXA-*r*-Red) copolymers may be attributed to the site isolation of the colored chromophores, the copolymer (TPA-*r*-Blue)-*b*-OXA (**7a**) was prepared for a control experiment. Copolymer **7a** was identical to the copolymer **7c** in terms of total MW = 100 kDa and was prepared from the same first block-containing blue iridium complexes within TPA, however, the OXA block did not include any monomer with the red iridium complex. Instead, the free red Ir(III) emitter small molecule, $Ir(pq)_2(tpys)$ (**4**), was added as a dopant into two different solutions of polymer **7a** in chlorobenzene to produce mixtures with **B**:**R** ratios of 10:0.5 and 10:1. The doped mixtures of **4** into polymer **7a** were spun-cast under identical conditions to produce a single layer device for a comparison to the bichromophoric diblock-copolymer polymer **7c** device having the same **B**:**R** ratio. Figure 4 shows the characteristics of three different devices. Device **D1** with a **B**:**R** ratio of 10:1 showed balanced dual emission while device **D3** prepared from a doped sample shows predominantly red emission at the same **B**:**R** ratio. In addition, a major portion of blue emission was quenched in device **D2** with an even lower **B**:**R** ratio of 10:0.5. As seen in Figure 4b, device **D1** with an EQE value of 1.5% performs significantly better than devices **D2** and **D3** with EQE values of 0.35% and 0.25%, respectively. The EQE values measured for devices **D2** and **D3** are very similar to those measured for low MW copolymers **5a** and **5b** for which no phase separation between the blocks, hence no chromophore site-isolation, was observed. Thus it appears that the nanophase separated morphology obtained by increasing block size in (TPA-*r*-Blue)-*b*-(OXA-*r*-Red) copolymers affords the site-isolation of chromophores necessary for improved device performance.

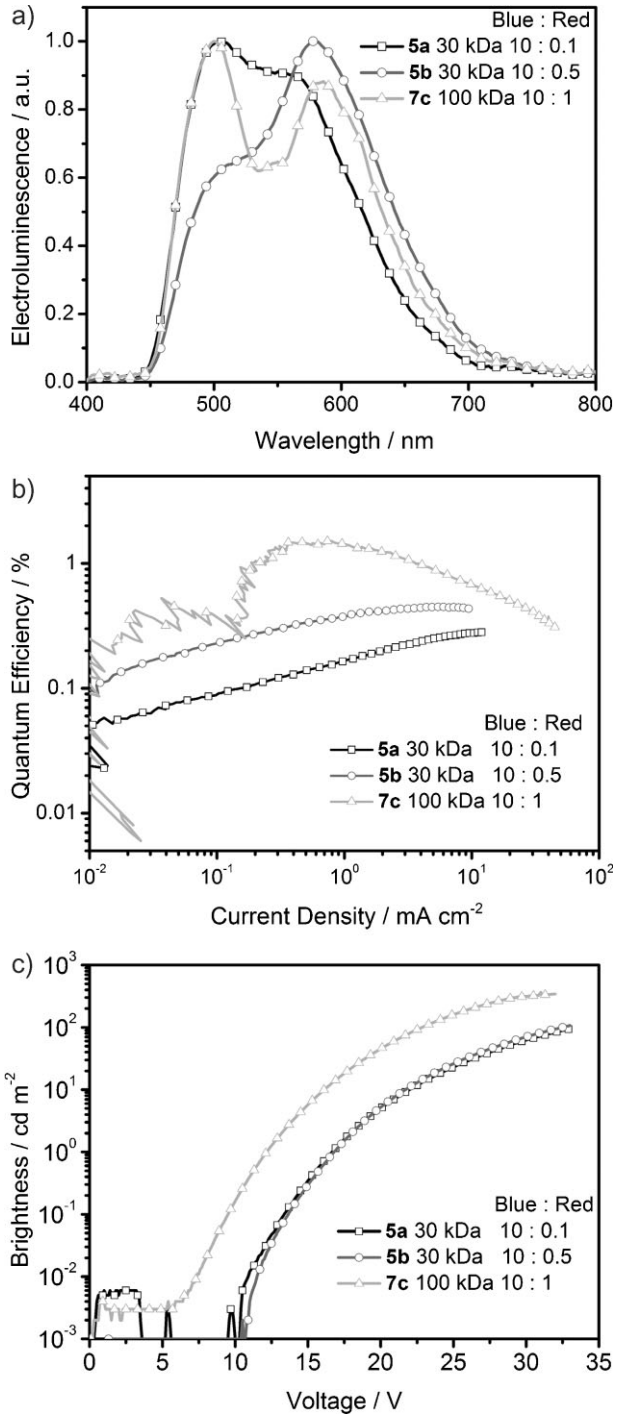

Figure 3. Device performance for selected copolymers **5a**, **6b**, **7c** a) Electroluminescence spectra; b) External quantum efficiency as a function of current density; c) Device brightness.

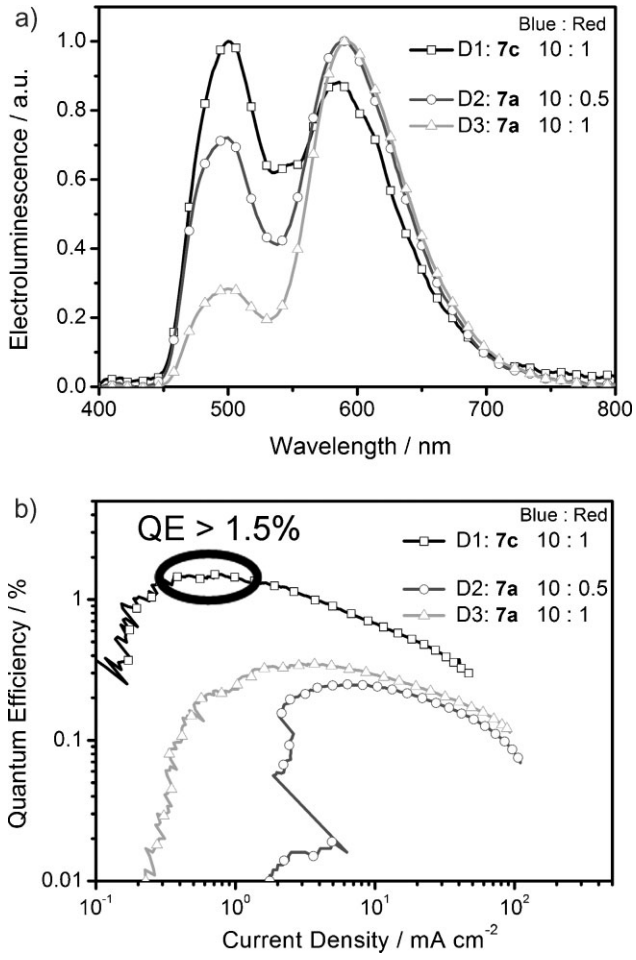

Figure 4. Comparison of (TPA-*r*-Blue)-*b*-(OXA-*r*-Red) polymer device to dopant system: a) Electroluminescence spectra; b) EQE of three different devices made of block copolymers having the same MW of 100 kDa, (**D1**: Single polymer system **7c** (MW = 100 kDa, B:R = 10:1), **D2**: Polymer **7a** mixed with red Ir dopants (MW = 100 kDa, B:R = 10:0.5), **D3**: Polymer **7a** mixed with red Ir dopants (MW = 100 kDa, B:R = 10:1)).

While overall performance of our block copolymer may appear to be relatively low, it must be emphasized that this was obtained with an extremely simple solution-cast device constituted of a single active layer directly sandwiched between anode and cathode. Thus the molecular approach towards site isolation described herein may be extended to other WOLED systems to improve their device efficiency. Since stable, bright, blue emission is still a limiting factor in high performance WOLEDs, our approach towards minimizing blue emission loss by suppressing unnecessary energy transfer to red dopants is versatile and broadly applicable.

Experimental

Synthesis: Details are provided in the Supporting Information.

Device Fabrication and Measurement: ITO coated glass substrates were cleaned through sonication in a soap solution, rinsing with deionized water, boiling in trichloroethylene, acetone, and ethanol then drying under nitrogen. The substrates were then placed under UV ozone for 10 minutes. All diblock copolymer films were prepared directly on top of the ITO substrate by spin-casting at 2000 RPM for 30 seconds from a 40 mg ml^{-1} solution of the polymer in chlorobenzene under inert atmosphere of argon. Following solution deposition of the polymer film a cathode consisting of 1 nm LiF (Aldrich, fused pieces 99.995%) and 100 nm Al (Alfa Aesar, purity > 99.99%) was deposited at a rate of 0.2 Å s^{-1} and 4 Å s^{-1} respectively, in a vacuum chamber below 3×10^{-6} Torr. OLEDs were formed at the 2×2 mm squares where the ITO and Al stripes intersect. The electrical

and optical intensity characteristics of the devices were measured with a Keithly 2400 sourcemeter/2000 multimeter coupled to a Newport 1835-C optical meter, equipped with a calibrated UV-818 Si photodetector. Only light emission from the front face of the device was collected and used in subsequent efficiency calculations. The EL spectra were measured on a USB4000 Miniature Fiber Optic Spectrometer.

TEM and GISAXS Measurement: The morphology of bulk sample as well as the thin film of (TPA-*r*-Blue)-*b*-(OXA-*r*-Red) polymers was investigated by TEM and GISAXS measurements. For Figure 2a–c, the thick film of (TPA-*r*-Blue)-*b*-(OXA-*r*-Red) polymers was prepared by dropcasting from a 40 mg ml^{-1} solution of the polymer in chlorobenzene. Samples were annealed at 230 °C during 3 days, then at 190 °C during 1 day and cooled slowly down to room temperature under vacuum. The bulk sample was microtomed into 50 nm thick film and sequentially stained by RuO_4 0.5% aqueous solution for 25 min to produce the contrast between (TPA-*r*-Blue) and (OXA-*r*-Red) blocks. A sample for Figure 2d was prepared using a slightly higher concentration of polymer to produce a thicker film. The films were prepared by spincasting from chlorobenzene onto NaCl substrate and then transferred to the epoxy substrate. The sample was microtomed into 50 nm thick film, followed by RuO_4 vapor staining for 25 min. The morphology of cross-sectioned bulk and thin film samples was observed by FEI Tecnai operated at 200 kV. For GISAXS measurements, samples were prepared on Si substrate under identical condition as the devices were prepared. GISAXS measurements were performed on beamline 7.3 at the Advanced Light Source at the Lawrence Berkeley National Laboratory. The scattering profiles were collected on an ADSC Quantum CCD detector. Incidence angle (~0.15°) was carefully chosen to allow for complete penetration of X-ray into the polymer film. The domain spacings of as-spuncast (TPA-*r*-Blue)-*b*-(OXA-*r*-Red) polymers in a thin film were extracted from scattered peak in in-plane direction of GISAXS images.

Acknowledgements

D. A. P. and B. J. K. contributed equally to this work. This work was performed with support by the Office of Science, Office of Basic Energy Sciences, of the U.S. Department of Energy under Contract No. DE-AC0205CH11231 for the Plastics Electronics Program at Lawrence Berkeley National Laboratory. Use of some facilities of the Molecular Foundry at LBNL is also acknowledged. The authors thank Dr. Alexander Hexemer, Mr. Eliot Gann and Dr. Cheng Wang for the help in GISAXS measurements at Advanced Light Source, which is supported by the U.S. Department of Energy under Contract No. DE-AC02-05CH11231. Supporting Information is available online from Wiley InterScience or from the author.

Received: May 1, 2009
Accepted July 9, 2009
Published online: September 3, 2009

[1] M. A. Baldo, D. F. O'Brien, Y. You, A. Shoustikov, S. Sibley, M. E. Thompson, S. R. Forrest, *Nature* **1998**, *395*, 151.
[2] D. F. O'Brien, M. A. Baldo, M. E. Thompson, S. R. Forrest, *Appl. Phys. Lett.* **1999**, *74*, 442.
[3] M. S. Arnold, G. J. McGraw, S. R. Forrest, R. R. Lunt, *Appl. Phys. Lett.* **2008**, *92*, 053301.
[4] H. Kanno, R. J. Holmes, Y. Sun, S. Kena-Cohen, S. R. Forrest, *Adv. Mater.* **2006**, *18*, 339.
[5] G. Parthasarathy, G. Gu, S. R. Forrest, *Adv. Mater.* **1999**, *11*, 907.
[6] Y. Sun, S. R. Forrest, *Appl. Phys. Lett.* **2007**, *91*, 263503.
[7] S. Tokito, T. Lijima, T. Tsuzuki, F. Sato, *Appl. Phys. Lett.* **2003**, *83*, 2459.
[8] Y. Sun, N. C. Giebink, H. Kanno, B. Ma, M. E. Thompson, S. R. Forrest, *Nature* **2006**, *440*, 908.
[9] M. Berggren, O. Inganas, G. Gustafsson, J. Rasmusson, M. R. Andersson, T. Hjertberg, O. Wennerstrom, *Nature* **1994**, *372*, 444.
[10] J. Liu, X. Guo, L. J. Bu, Z. Y. Xie, Y. X. Cheng, Y. H. Geng, L. X. Wang, X. B. Jing, F. S. Wang, *Adv. Funct. Mater.* **2007**, *17*, 1917.
[11] J. Liu, Z. Y. Xie, Y. X. Cheng, Y. H. Geng, L. X. Wang, X. B. Jing, F. S. Wang, *Adv. Mater.* **2007**, *19*, 531.
[12] J. Luo, X. Li, Q. Hou, J. B. Peng, W. Yang, Y. Cao, *Adv. Mater.* **2007**, *19*, 1113.
[13] G. L. Tu, C. Y. Mei, Q. G. Zhou, Y. X. Cheng, Y. H. Geng, L. X. Wang, D. G. Ma, X. B. Jing, F. S. Wang, *Adv. Funct. Mater.* **2006**, *16*, 101.
[14] F. Chen, Y. Yang, M. E. Thompson, J. Kido, *Appl. Phys. Lett.* **2002**, *80*, 2308.
[15] P. Shih, C. Shu, Y. Tung, Y. Chi, *Appl. Phys. Lett.* **2006**, *88*, 251110.
[16] Y. Xu, X. Zhang, J. Peng, Q. Niu, Y. Cao, *Semicond. Sci. Technol.* **2006**, *21*, 1373.
[17] J. Liu, B. Gao, Y. Cheng, Z. Xie, Y. Geng, L. Wang, X. Jing, F. Wang, *Macromolecules* **2008**, *41*, 1162.
[18] M. Park, J. Lee, J. Park, S. K. Lee, J. Lee, H. Chu, D. Hwang, H. Shim, *Macromolecules* **2008**, *41*, 3063.
[19] J. X. Jiang, Y. H. Xu, W. Yang, R. Guan, Z. Q. Liu, H. Y. Zhen, Y. Cao, *Adv. Mater.* **2006**, *18*, 1769.
[20] A. W. Freeman, S. C. Koene, P. R. L. Malenfant, M. E. Thompson, J. M. J. Fréchet, *J. Am. Chem. Soc.* **2000**, *122*, 12385.
[21] P. Furuta, J. Brooks, M. E. Thompson, J. M. J. Fréchet, *J. Am. Chem. Soc.* **2003**, *125*, 13165.
[22] M. R. Bockstaller, R. A. Mickiewicz, E. L. Thomas, *Adv. Mater.* **2005**, *17*, 1331.
[23] F. S. Bates, G. H. Fredrickson, *Phys. Today* **1999**, *52*, 32.
[24] B. J. Kim, J. Bang, C. J. Hawker, E. J. Kramer, *Macromolecules* **2006**, *39*, 4108.
[25] J. Bang, S. H. Kim, E. Drockenmuller, M. J. Misner, T. P. Russell, C. J. Hawker, *J. Am. Chem. Soc.* **2006**, *128*, 7622.
[26] B. J. Kim, G. H. Fredrickson, C. J. Hawker, E. J. Kramer, *Langmuir* **2007**, *23*, 7804.
[27] K. Sivula, Z. T. Ball, N. Watanabe, J. M. J. Fréchet, *Adv. Mater.* **2006**, *18*, 206.
[28] T. F. Jaramillo, S. H. Baeck, B. R. Cuenya, E. W. McFarland, *J. Am. Chem. Soc.* **2003**, *125*, 7148.
[29] J. I. Lee, S. H. Cho, S. Park, J. K. Kim, J. K. Kim, J. Yu, Y. C. Kim, T. P. Russell, *Nano Lett.* **2008**, *8*, 2315.
[30] M. R. Bockstaller, E. L. Thomas, *J. Phys. Chem. B* **2003**, *107*, 10017.
[31] J. Y. Cheng, C. A. Ross, V. Z. H. Chan, E. L. Thomas, R. G. H. Lammertink, G. J. Vancso, *Adv. Mater.* **2001**, *13*, 1174.
[32] B. Ma, B. J. Kim, L. Deng, D. A. Poulsen, M. E. Thompson, J. M. J. Fréchet, *Macromolecules* **2007**, *40*, 8156.
[33] T. Förster, *Discuss. Faraday Soc.* **1959**, *27*, 7.
[34] N. J. Turro, *Modern Molecular Photochemistry;*, University Science Books, Sausalito, CA **1991**.
[35] P. T. Furuta, L. Deng, S. Garon, M. E. Thompson, J. M. J. Fréchet, *J. Am. Chem. Soc.* **2004**, *126*, 15388.
[36] X. Y. Wang, R. N. Prabhu, R. H. Schmehl, M. Weck, *Macromolecules* **2006**, *39*, 3140.
[37] K. Zhang, Z. Chen, Y. Zou, C. Yang, J. Qin, Y. Cao, *Organometallics* **2007**, *26*, 3699.
[38] J. Langecker, M. Rehahn, *Macromol. Chem. Phys.* **2008**, *209*, 258.
[39] C. Adachi, R. C. Kwong, P. Djurovich, V. Adamovich, M. A. Baldo, M. E. Thompson, S. R. Forrest, *Appl. Phys. Lett.* **2001**, *79*, 2082.
[40] Y. You, S. Y. Park, *J. Am. Chem. Soc.* **2005**, *127*, 12438.
[41] J. H. Seo, I. J. Kim, Y. K. Kim, Y. S. Kim, *Jpn. J. Appl. Phys.* **2008**, *47*, 6987.
[42] F. S. Bates, G. H. Fredrickson, *Annu. Rev. Phys. Chem.* **1990**, *41*, 525.